Water Contamination Effect on Liquid Acetonitrile/TiO 2 Anatase (101) Interface for Durable Dye-Sensitized Solar Cell

ARTICLE *in* THE JOURNAL OF PHYSICAL CHEMISTRY C · SEPTEMBER 2011

Impact Factor: 4.77 · DOI: 10.1021/jp206910f

4 AUTHORS, INCLUDING:

Masato Sumita
National Institute for Materials Science
35 PUBLICATIONS **312** CITATIONS
SEE PROFILE

Keitaro Sodeyama
Kyoto University
41 PUBLICATIONS **435** CITATIONS
SEE PROFILE

THE JOURNAL OF PHYSICAL CHEMISTRY C

ARTICLE

pubs.acs.org/JPCC

Water Contamination Effect on Liquid Acetonitrile/TiO_2 Anatase (101) Interface for Durable Dye-Sensitized Solar Cell

Masato Sumita,[†] Keitaro Sodeyama,[†,‡] Liyuan Han,[‡,§] and Yoshitaka Tateyama[*,†,‡,∥]

[†]Nano-System Computational Science Group, Nano-System Organization Unit, International Center for Materials Nanoarchitectonics (MANA), National Institute for Materials Science (NIMS), 1-1 Namiki, Tsukuba, Ibaraki 305-0044, Japan

[‡]CREST, Japan Science and Technology Agency (JST), 4-1-8 Honcho, Kawaguchi, Saitama 333-0012, Japan

[§]Photovoltaic Materials Unit, NIMS, 1-2-1 Sengen, Tsukuba, Ibaraki 305-0047, Japan

[∥]PRESTO, JST, 4-1-8 Honcho, Kawaguchi, Saitama 333-0012, Japan

Supporting Information

ABSTRACT: We have investigated the structural and electronic properties of liquid acetonitrile (MeCN)/TiO_2 anatase (101) interfaces involving a water molecule in order to analyze effect of ubiquitous water contamination in the typical electrolyte solution on the durability of dye-sensitized solar cell (DSSC), by using density-functional molecular dynamics simulations at room temperature. Our results show that H_2O does not dive into the unbound Ti_{5C} sites on the (101) surface kinetically, once the coverage of MeCN is saturated ($\Theta \approx 0.6$). However, H_2O adsorption through hydrogen bond with surface O_{2C} sites, not a Ti_{5C} site, is found the most stable if MeCN solvent is introduced to H_2O-preadsorbed TiO_2 anatase (101) surface. This no-adsorption character of Ti_{5c} site in the aprotic solvent MeCN is in stark contrast to the case where the (101) surface is immersed by H_2O layer or liquid H_2O. The adsorbed H_2O molecule via the hydrogen bond between O_{2C} and H_W has its $1b_1$ orbital at an energy just below the valence band maximum of TiO_2. Therefore, this H_2O has a sufficient possibility to become a cation radical by capturing hole generated by irradiation, which may attack the dye molecules toward the desorption. We thus demonstrate that removing H_2O from the anatase (101) surface prior to introduction of the MeCN electrolyte solution is crucial to make the DSSCs more durable and efficient.

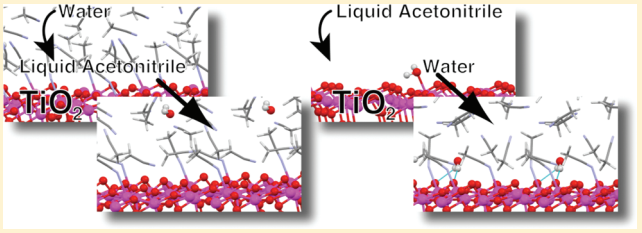

1. INTRODUCTION

Dye sensitized solar cell (DSSC)[1−3] is a promising alternative to the conventional silicon-based photovoltaic devices from the viewpoint of efficiency and cost performance. In DSSC, a sensitizing dye molecule adsorbed on a semiconductor surface (usually nanocrystal anatase TiO_2) absorbs light effectively and transfers the excited electron to the conduction band of the semiconductor anode. The electron getting through the circuit is transferred to redox species in the electrolyte solution on the counter electrode (cathode) and eventually regenerates the oxidized dye by reduction. The high efficiency of visible light absorbance of low-cost dye molecules is a key advantage of DSSC compared to the conventional Si-based cells.[4] Solar energy conversion efficiency of over 11% was achieved by Ru-polypirysil dyes,[5,6] whereas further improvement of the efficiency and durability is necessary for an alternative to the conventional cells. For this purpose, considerable research to understand and improve this photoabsorption stage and the following electron transfer have been conducted over the last few decades, although the atomistic pictures have not yet been fully understood.

Recently, however, contribution of the electrolyte solution, namely redox species, counterions, additives, and solvents, has attracted much attention as well, because the electrolyte may have a certain effect on the critical processes for the DSSC performance such as back electron transfer from the anode, regeneration by the redox species, as well as adsorption stability of the dye molecules. In fact, studies on the electrolyte dependence of the DSSC performance suggest that high efficiency is achieved by immersing the anode in aprotic solvent like MeCN[7,8] which has unique characteristics, e.g., high dielectric constant, and solubilization of many inorganic and organic materials.[9,10] Transient adsorption (TA) spectroscopy of the black dye on the TiO_2 surface shows that the MeCN immersion bring about 50% increase of the signal compared to in-vacuo,[7] indicating increase of electron injection efficiency with introduction of MeCN. However, protic solvents like water and alcoholic solvents show rather low short-circuit photocurrent density (J_{SC}) in comparison with the aprotic ones,[8,11] probably because the presence of water decreases the injection efficiency of the dye.[12] It is also found that J_{SC} using protic solvents are decreased drastically with increasing irradiation time, which is attributed to desorption of the dye molecules[7] (probably the products produced from protic solvent by light irradiation may attack the dye molecules[13]). These obviously show the efficiency of aprotic MeCN and the

Received: July 20, 2011
Revised: September 1, 2011
Published: September 02, 2011

degradation effect of ubiquitous water for the electrolyte solution in DSSC.

Some theoretical investigations of the solvent effect have been recently carried out as well. Force field calculation exhibits the TiO_2 anatase (101) surface fully covered by MeCN, where all undercoordinated Ti sites [5-fold coordinated Ti (Ti_{5C})] on the (101) surface are covered by MeCN (TiO_2 surface is passivated by MeCN)[14] even though there is an O vacancy on the (101) surface.[15] With this result, Schiffmann et al. suggests that back electron transfer, leading to decrease of the net efficiency, is reduced by preventing redox species (ex. tri-iodide) from approaching to the surface.[16] This implies that the interface structure between the solvent and TiO_2 surface strongly influences the performance of DSSCs.

In addition to the bulk solvent, it is important to consider contamination in the synthesis processes of DSSCs. The low cost merit of DSSC is attributed to the fact that the synthesis can be done under ambient condition, namely in the air. After the treatment of the TiO_2 nanocrystal surfaces, dye adsorption is carried out and followed by introduction of the electrolyte solvent in the air. Therefore, involving ubiquitous H_2O molecules in the DSSC system is highly possible, and it is so demanding to prevent H_2O from mixing into the DSSC system during the fabrication. Since the water usually degrades the performance, this mixing effect is also a crucial issue for the improvement of efficiency and durability of DSSCs.

In this respect, we investigate the effect of ubiquitous water contamination in the MeCN electrolyte solution, a typical and most effective solvent in DSSC, on the TiO_2 surface, in this work. With first-principles molecular dynamics simulations at room temperature, we examine the equilibrium structural and electronic properties of the liquid MeCN/TiO_2 anatase (101) surface including a water molecule, corresponding to a typical concentration of water contamination. Using clean and H_2O-preadsorbed (101) surfaces, we obtain several metastable configurations and examine the relationship between the electronic band structure of TiO_2 and the water-originated states. (Here we found H_2O adsorption to TiO_2 surface in an unusual way.) Analysis of the possibility of dye desorption is made on the basis of these electronic states, although the dye molecule is not included in the present calculations. We finally suggest how to decrease possible H_2O-induced degradation of the DSSC performance.

2. COMPUTATIONAL DETAILS

All first-principles molecular dynamics simulations are carried out using density functional theory (DFT) methods implemented in CPMD.[17] Total energies were calculated at the Γ point in a super cell approach by using BLYP generalized gradient corrected exchange-correlation functional. The Kohn−Sham orbitals were expanded by plane wave basis set up to the energy cutoff of 70 Ry. Troullier-Martin type norm-conserving pseudopotentials are used for all atoms. In particular, Ti pseudopotential utilizes the nonlinear core correction approach that includes 3*d* and 4*s* in the valence electrons.[18]

For dynamics, we use Nosé-Hoover thermostat[19] with the temperature of 300 K for NVT ensemble. The time step is set to 0.12 fs, and 0.27 u is used for the fictitious mass for electrons in Car−Parrinello dynamics.[20] After equilibration with a couple of picoseconds (ca. 7 ps), we obtained the equilibrium trajectories, which are used to carry out sampling.

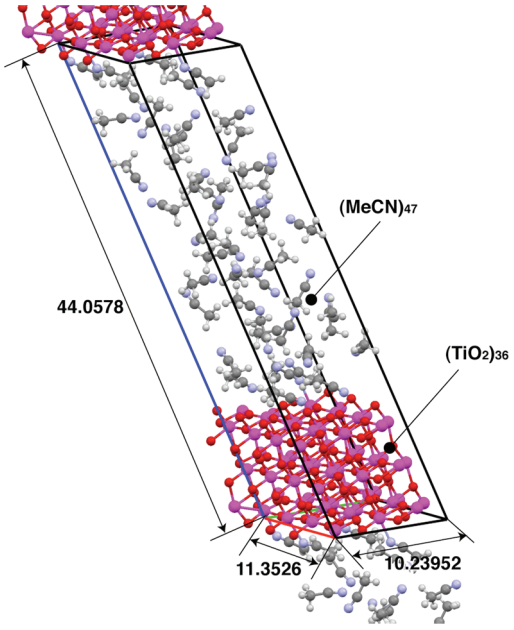

Figure 1. The unit cell we use in this work. The illustrated structure is a snapshot in the equilibrium trajectories of TiO_2 anatase (101) surface/bulk MeCN.

We used the (3 × 1) anatase (101) surfaces, corresponding to $(TiO_2)_{36}$ composition (see Figure 1). The experimental lattice parameters are used: We use a monoclinic cell with the parameters of 11.3526 × 10.23952 × 44.05780 Å and α = 111.689° for the anatase (101)/bulk MeCN system (see Figure 1). We had comprehensively examined the structural dependence on the lattice parameters and the thickness of slab.[21] Then, we concluded that the simulation with the experimental parameters gives reasonable results.

MeCN molecules are stuffed in the open space between the TiO_2 slabs so that the density of MeCN becomes about 0.78 g/cm^3.[22] Both top and bottom sides of the slab are activated as shown in Figure 1. We have checked the validity of the present model of bulk MeCN by radial distribution functions (RDFs) between nitrogen and carbon atoms in the MeCN region in the equilibrium trajectories. Figure 2 shows the density profiles of nitrogen and carbon atoms in MeCN molecules along vertical axis (*z*-axis). On the basis of this density profile, bulk MeCN molecules are classified to layers along the *z*-axis. N_A-C_A RDFs (Here under subscript "A" means the atoms originated from MeCN) of each layer are shown in Figure 3. The second peaks are shifted to a longer distance as moving from the third to the fifth layer. Although the RDF exhibits less density bulk MeCN exists in the fifth layer (3.54 Å) in comparison with the experimental result (3.45 Å)[9] and the previous calculation,[10] we believe that the MeCN part in the present systems well describes the bulk MeCN at the BLYP level.

3. RESULTS AND DISCUSSION

Before discussion about the interface between TiO_2 and bulk MeCN with H_2O, we have revisited the interface TiO_2/bulk MeCN by using full first-principles simulations. This simulation is necessary to get the equilibrium condition of the interface between TiO_2 and MeCN.

3.1. TiO_2/MeCN Interface. A snapshot of the equilibrium trajectory of the TiO_2/bulk MeCN interfaces is shown in Figure 4.

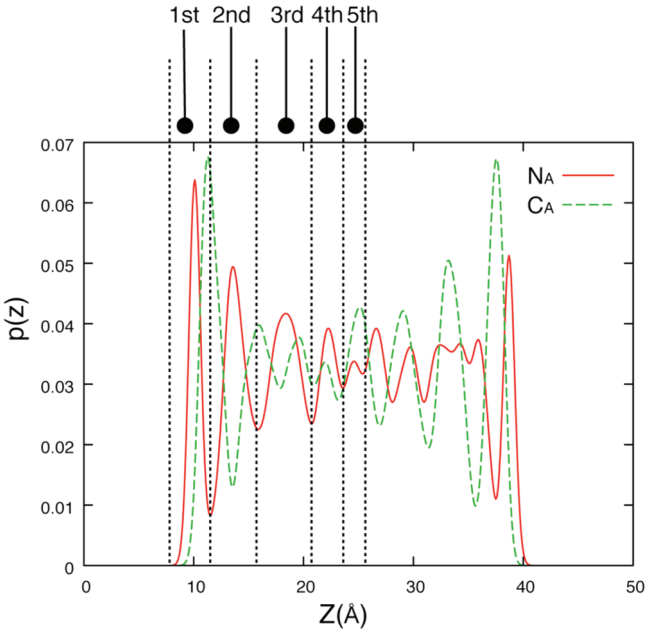

Figure 2. Normalized density profile, which is perpendicular to TiO_2 anatase (101) surface. Here, we define a Ti atom on the bottom of the slab as the origin. On the basis of this distribution function, we divide MeCN molecules into each layer, i.e., from a valley to the neighboring valley (divided by valleys). The first layer is composed of the MeCN molecules adsorbed to Ti_{5C}. The second layer consists of the MeCN molecules with the methyl groups directed to the surface.

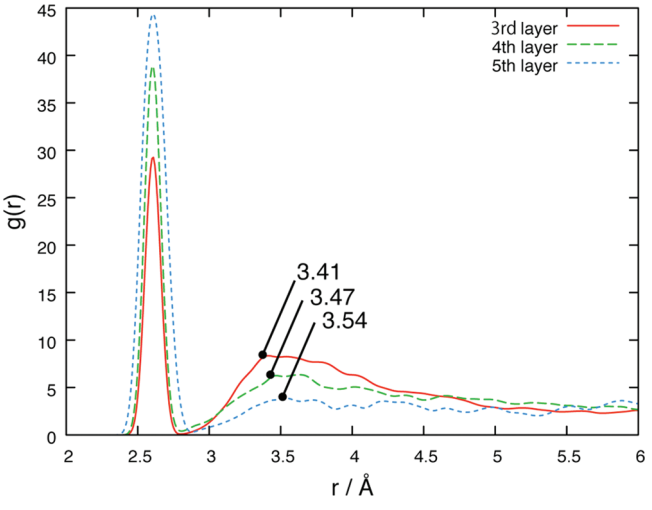

Figure 3. The radial distribution function from N_A to C_A of bulk MeCN in the third-fifth layer. The first peak is assigned to intramolecular N_A-C_A. The second peak denotes the intermolecular one.

Throughout the all equilibrium trajectory, the number of adsorbed MeCN molecule is 3.01×10^{16} molecules cm^{-2} (coverage $\Theta \approx 0.58$), which is the same number of adsorbed H_2O molecules in the case of TiO_2/bulk water.[21] In order to eliminate the initial structure dependence, we have carried out the MD calculation from the structure where the all Ti_{5C} are filled by MeCN as well, and confirmed that the number of adsorbed MeCN molecules does not alter at equilibrium. Hence, the situation where MeCN molecules fill all the Ti_{5C} sites (corresponding to $\Theta = 1$) is not possible. Accordingly, there are some Ti_{5C} sites that have possibility to interact with other molecules, even on the (101) surface passivated by MeCN molecules.

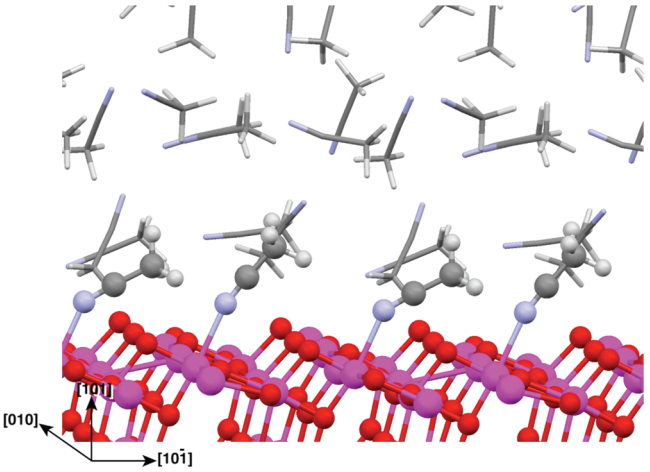

Figure 4. Snapshot in the equilibrium trajectory of the TiO_2/bulk MeCN interface. The TiO_2 surface and MeCN adsorbed to it are described by ball and stick model. The other MeCN molecules are described by capped stick model.

Table 1. Bond Length/Distance (in Å) Estimated by Radial Distribution Functions (RDFs) for Pure Acetonitrile (MeCN) and Three Metastable Configurations Found in This Work[a]

	pure MeCN	I	II	III
$Ti_{5C}-N_A$	2.38	2.35	2.35	2.37
$O_{2C}-H_A$	2.57	2.74	2.64	2.66
$Ti_{5C}-O_W$			4.03	2.34
$O_{2C}-H_W$			1.85	2.20
O_W-H_A		2.0−3.0	2.26	2.0−3.0
H_W-N_A		2.07	2.08	2.06

[a] See Figure 7 for the structures.

The average bond length of $Ti_{5C}-N_A$ is around 2.38 Å in the RDF between Ti_{5C} and N_A (Table 1), which is compatible with previous calculations.[14] Since MeCN is a rather long molecule, the tilt angle of adsorbed MeCN to the surface is important. That is, if MeCN is parallel to the surface, other molecules are sterically hindered from approaching the surface. Otherwise, other molecules may adsorb to the surface through MeCN layer. Schiffmann et al.[14] exhibited the distribution of the cosine of the angle between the surface normal and the MeCN dipole from the result of molecular dynamics based on force field. This quantity is not a direct measure to see whether MeCN is parallel to the surface or not. Then we have analyzed the distribution of the bond angle $Ti_{5C}-N-C$ (θ), which is shown in Figure 5. There are large three peaks. The first one is around 145°, the second one is around 150°, and the last one is around 165°. Adsorbed MeCN molecules have a considerably "standing" structure, although the structure where Ti_{5C}, N_A, and C_A are along the straight line (θ = 180°) is rare. This tendency appears even in vacuo. The calculations about the anatase (101)/ one MeCN molecule in vacuo also indicate that there are minima around θ = 150° (see Supporting Information). This is likely to be attributed to slight charge transfer between MeCN and the surface, which could

dx.doi.org/10.1021/jp206910f |J. Phys. Chem. C 2011, 115, 19849–19855

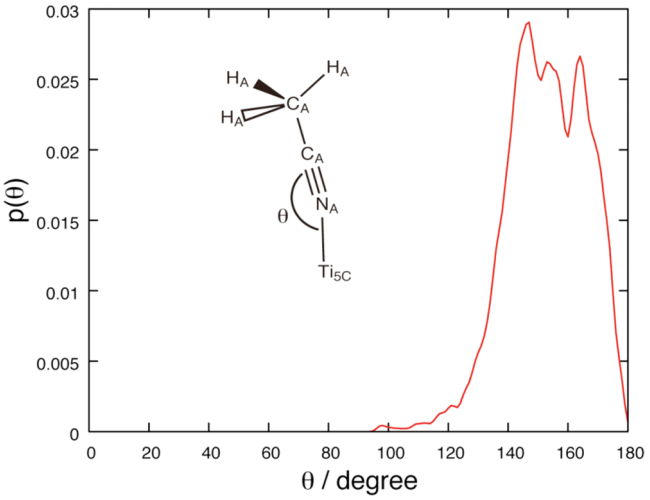

Figure 5. Normalized distribution function of the bond angle of $Ti_{5C}-N_A-C_A$. There are three peaks. The first is around 140°. The next is 150°. The last one is 170°. The structure where Ti_{5C}, N_A, and C_A are along the straight line ($\theta = 180°$) is rare.

perturb the *sp* hybrid orbital of N_A. In consequence, the (101) surface on which MeCN molecules adsorb has a lot of space sterically and potentially active sites (Ti_{5C}) still remain. Therefore, in this TiO_2/MeCN system, other molecules possibly enter into these spaces.

The previous calculation[14] claimed that MeCN can adsorb through the methyl group directing to the surface via the hydrogen bond between hydrogen atom of the methyl group and two coordinated oxygen atom (O_{2C}) on the surface. These MeCN molecules correspond to the second layer in Figure 2. Since the estimated distance of H_A and O_{2C} is 2.57 Å, it is regarded that the weak hydrogen bond is formed between them.[23]

It is noteworthy to investigate the electronic effect by MeCN to the TiO_2 anatase (101) surface. The previous calculation based on the extended Hückel method[13] showed projected density of state (PDOS) to clarify the influence of O-vacancy on the surface in bulk MeCN. However, there is no prediction about the influence by liquid MeCN itself. Here, we show the electronic effect by MeCN to the TiO_2 anatase (101) surface.

Mulliken population analysis indicates that N_A atoms of the MeCN adsorbed to the surface become more electron rich than that of bulk MeCN. That is, the charge of N_A is −0.226 a. u., and that of N_A in bulk MeCN is −0.194 a.u. Furthermore, Ti_{5C} on which MeCN is adsorbed via $Ti_{5C}-N_A$ bond has more positive charge than bare Ti_{5C}. Hence, this back-donation effect from Ti_{5C} to N_A. Because electrons are slightly withdrawn from the surface, the top of the valence band of the TiO_2 slab is likely to be shifted upward. This effect is also reflected in the projected density of states (PDOSs) shown in Figure 6. Comparing the PDOS of the (101) surface in vacuo and in MeCN bulk clarifies that the energy gap (energy difference between conduction band minimum and valence band maximum) in MeCN bulk is smaller than that in vacuo by 0.07 eV at average of three snapshots.

3.2. TiO_2/MeCN Interface Contaminated by H_2O. After getting the equilibrium structure between TiO_2/bulk MeCN, we put into one H_2O molecule by replacing one MeCN molecule [$(MeCN)_{46}$ and H_2O], which exists in third layer. The density of water corresponds to about 0.5 M, comparable to the real system.[11] One snapshot is shown in Figure. 7 (structure **I**) after the energetic

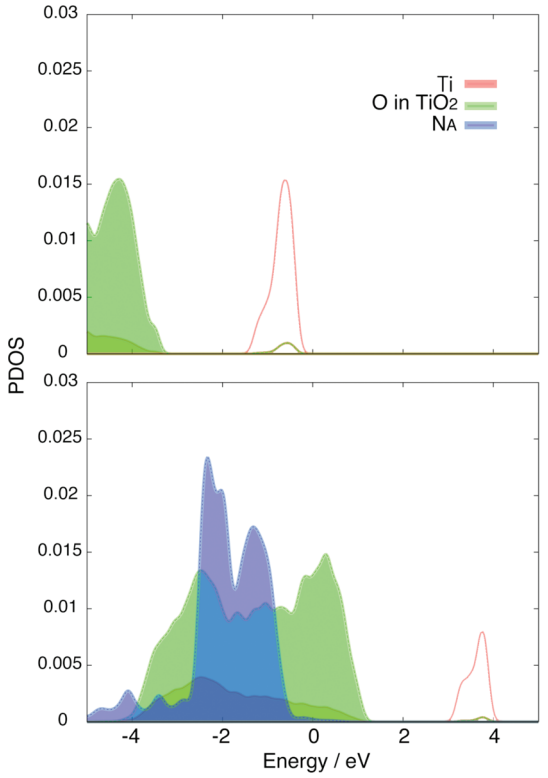

Figure 6. Projected density of state (PDOS) of each system. Top: TiO_2 anatase (101) surface in vacuo. Bottom: TiO_2 anatase (101) surface in bulk MeCN. Valence bands are filled by the corresponding colors.

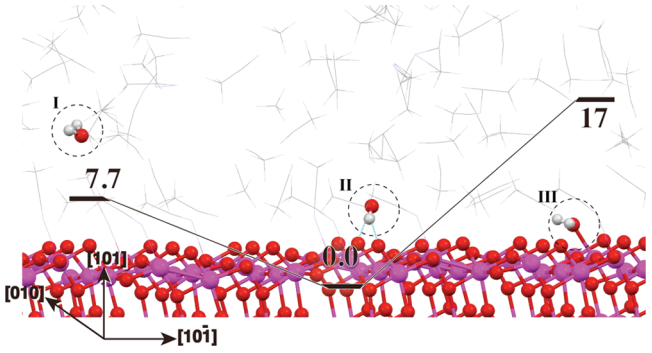

Figure 7. Snapshots of structures **I**, **II**, and **III**, metastable structures in the TiO_2/bulk MeCN interfaces contaminated by H_2O. **I**: H_2O molecule exists in bulk MeCN. **II**: the most stable structure of H_2O molecule in bulk MeCN i.e., and H_2O adsorbed on the TiO_2 surface via strong hydrogen bond between H_W and O_{2C}. **III**: H_2O molecule is adsorbed on the TiO_2 surface via the bond between O_W and Ti_{5C} with their energy diagram (in kcal mol^{-1}). The values of the energy are estimated by Figure 8 and Table 2. The mean energy is also shown.

equilibrium condition achieved. In spite of a lot of space on the interface of TiO_2/bulk MeCN, H_2O cannot dive into the (101) surface. According to the RDF between H_W/O_W (here under subscript "W" means the atoms originated from water molecule) and the surface (i.e., Ti_{5C}, O_{2C}), the H_2O molecule is more than 5.0 Å apart from the surface. The MeCN molecules prevent H_2O from approaching to the surface by making the hydrogen bond between H_W and N_A or interaction between O_W and H_A. The distances of H_W-N_A and O_W-H_A are estimated at 2.07 Å and

dx.doi.org/10.1021/jp206910f |J. Phys. Chem. C 2011, 115, 19849–19855

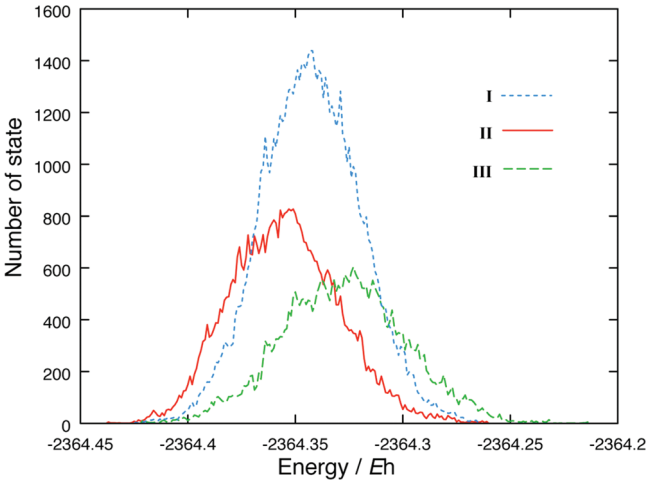

Figure 8. Histograms of total energies while the energetic equilibrium condition of structure **I** (TiO_2 anatase (101) surface with H_2O in bulk MeCN), **II** (TiO_2 anatase (101) surface with H_2O adsorbed to the surface via hydrogen bonds between H_W and O_{2C}), and **III** (TiO_2 anatase (101) surface with H_2O adsorbed to the surface via bond between O_W and Ti_{5C}) shown in Figure 7.

Table 2. Mean Total Energy and Standard Deviation of First-Principles Molecular Dynamics in the Equilibrium Conditions for Each Metastable Configuration

system	mean energy (E_h)	standard deviation (E_h)	relative mean energy (kcal mol^{-1})
I	−2364.34208	0.022957	7.68
II	−2364.35432	0.025073	0.00
III	−2364.32715	0.028713	17.05

2.0−3.0 Å, respectively, in the RDFs (See Supporting Information for detailed structure around H_2O). This indicates that, once TiO_2 (101) surface is passivated by MeCN, H_2O molecule cannot adsorb on the (101) surface through MeCN layer. This means that electronic interaction rather than steric interaction between MeCN and H_2O prevent H_2O from diving into the TiO_2 surface.

Assuming the condition in which water molecules are adsorbed on the surface before the anatase TiO_2 film immersed into MeCN solvent, we have made the optimized TiO_2 slab on which one water molecule is adsorbed in vacuo (see Supporting Information). Then, we carried out the molecular dynamics after dipping this slab into 46 MeCN molecules. $Ti_{5C}-O_W$ bond is kept while about 4 ps after energetic equilibrium achieved. Structure **III** of Figure 7 shows this structure. Structure **III** is exactly a local minimum because the histogram of total energy in Figure 8 exhibits the broad Gauss distribution whose peak is at approximately −2364.32 E_h. However, this structure is found as an intermediate later on. After 5 ps, the peak position is shifted to the energetically lower side at approximately −2364.35 E_h, where the $Ti_{5C}-O_W$ bond is broken keeping the hydrogen bonds between O_{2C} and H_W. A snapshot is shown in Figure 7 (structure **II**). Since the numbers of the atoms in structure **I**, **II**, and **III** are the same, we can compare energies between them. The peak of structure **I** in Figure 8 is at approximately −2364.34 E_h. Therefore, the most stable structure seems to be **II**.

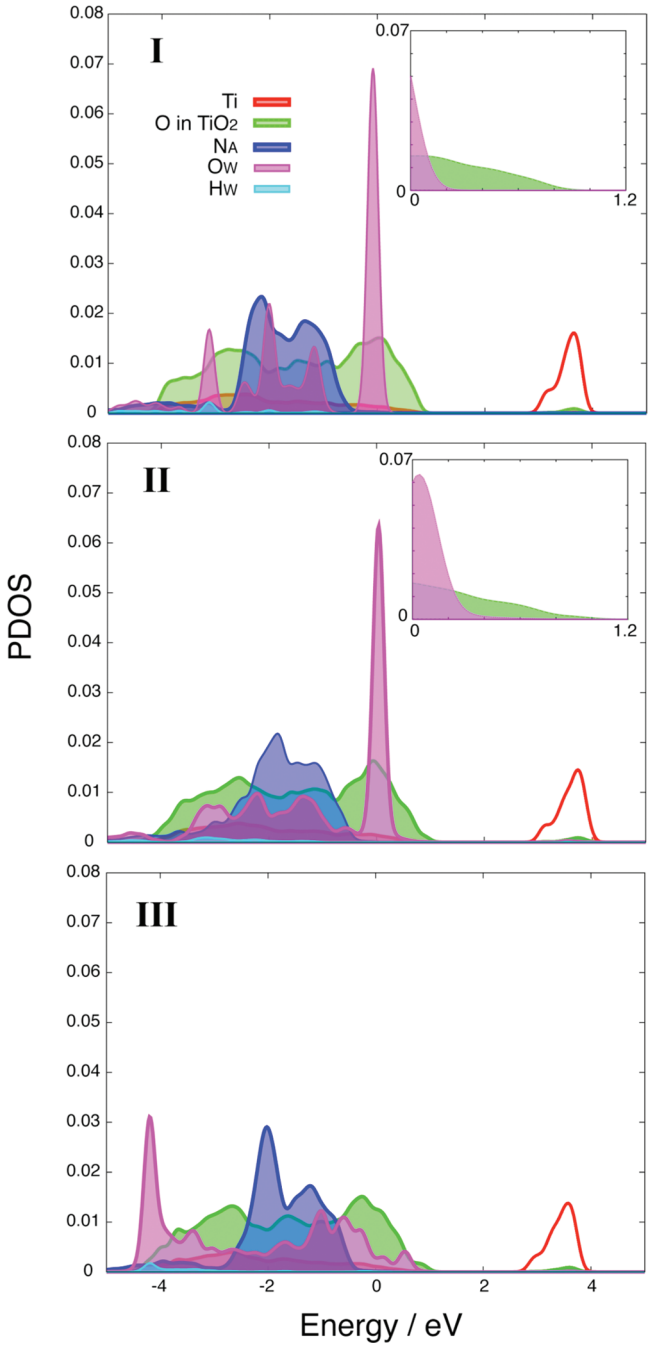

Figure 9. Projected density of states (PDOSs) of each system: **I** (H_2O in bulk MeCN), **II** (H_2O adsorbed to the surface via the bond between Ti_{5C} and O_W), and **III** (H_2O adsorbed to the surface via the hydrogen bond between O_{2C} and H_W). Valence bands are filled by the corresponding colors. Insets are the magnification view in the area from 0.0 to 1.2 eV.

More quantitatively, mean energies and standard deviations are tabulated in Table 2. Because all of the values of standard deviation are within 0.028 E_h (18 kcal mol^{-1}), total energies are distributed around their mean values. Furthermore, each peak of the histogram of total energy in Figure 8 agrees with the mean energy. Therefore, these allow us to compare the mean energy of each state. Structure **III**, which seems to be an intermediate structure, is the most unstable state and lies 17 kcal mol^{-1} above

Table 3. Averaged Mulliken Charges (in a.u.) of Atoms in the Anatase (101) Surface/Bulk MeCN with H_2O Systems

	pure MeCN	I	II	III
N_A (Adsorbed)	−0.226	−0.228	−0.229	−0.226
N_A	−0.194	−0.192	−0.192	−0.189
Ti_{5C} (covered by MeCN)	2.631	2.603	2.631	2.603
O_W		−0.498	−0.466	−0.503
H_W		0.3475	0.307	0.336
Ti_{5C} (covered by H_2O)				2.624
Ti_{5C} (bare)	2.610	2.587	2.601	2.632

structure **II**. Structure **II** is the most stable state and lies approximately 8.0 kcal mol^{-1} below water in bulk MeCN. Figure 7 shows the energy diagram between the systems characterized by H_2O configurations.

Previous substantial studies[21,25,26] about H_2O on the (101) surface have shown that Ti_{5C} is the adsorption site for H_2O. In the condition where a few or bulk H_2O are on the surface, O_W binds to Ti_{5C} in the company with the hydrogen bonds between H_W and O_{2C}. According to our preliminary calculation of one molecule on the (101) surface in vacuo, the adsorption energy of H_2O on the (101) surface is 11.15 kcal mol^{-1} while that of MeCN is 9.54 kcal mol^{-1}. Thus, though the adsorption energy of H_2O onto the surface is larger than that of MeCN in vacuo, $Ti_{5C}-O_W$ bond is broken due to the solvation effect of MeCN. The usual $Ti_{5C}-O_W$ bond length is approximately 2.11−2.28 Å,[21,25,26] while the $Ti_{5C}-O_W$ bond in the intermediate structure **III** in bulk MeCN is estimated at 2.34 Å. Hence, MeCN considerably weakens the $Ti_{5C}-O_W$ bond. Therefore, Ti_{5C} is not the adsorption site for H_2O in the MeCN solvent. However, the estimated $O_{2C}-H_W$ bond length in the RDF is 1.85 Å, which is longer than that in the system of anatase TiO_2/bulk H_2O (1.78 Å).[21] Hence, the interaction between H_2O and the (101) surface is weakened in MeCN solvent due to no network of hydrogen bond. However, our molecular dynamics simulation indicates that it is hard to remove adsorbed H_2O molecule on the interface once it is adsorbed on the anatase (101) surface. Indeed, these hydrogen bonds between O_{2C} and H_W are kept even when we increase the simulation temperature to 400 K. This result agrees with the experimental suggestion that water interact with the TiO_2 surface strongly in the DSSC system.[24]

In order to understand the electronic effect of the water molecule on the electronic states, we analyze PDOS and Mulliken charge population. Figure 9 shows typical PDOSs of the three metastable states of water-contaminated MeCN/TiO_2 interfaces. The valence bands of MeCN and H_2O appear around more than 0.08 eV below the valence band top of TiO_2. The energy gaps in structure **I** and **II** are approximately 2.23 eV, comparable to the system of TiO_2/pure bulk MeCN. Only short-lived structure **III** has smaller energy gap (2.18 eV). Therefore, the existence of 0.5 M H_2O does not have significant influence to the whole electronic structure of the TiO_2 in bulk MeCN. However, the states associated with H_2O is different depending on the H_2O configurations. In the case of **I**, a very sharp peak whose origin is the $1b_1$ orbital of H_2O, the $2p$ orbital of O_W, appears around −0.5 eV as shown in Figure 9. The edge of this peak lies at 0.82 eV below the top of the valence band. Probably, this H_2O is the same as that in the isolated condition. This water molecule might not be harmful to DSSC systems in spite of the $1b_1$ state position because there is a distance between O_W and the surface, making the transfer probability of photogenerated hole small.

In the PDOS of structure **III**, the $1b_1$ orbital of H_2O is broaden in energy compared to those of **I** and **II** due to the interaction O_W and Ti_{5C}. This represents the interaction between $2p$ orbital of O_{2C} and $3d$ orbital of Ti_{5C}. If this structure **III** were energetically most stable, then this water molecule would be the most harmful to the DSSC system. Fortunately, the lifetime of this sort of water is not long.

Similar to the PDOS of **I**, PDOS of structure **II** shows a sharp peak to the $2p$ orbital of O_W. The edge of this peak lies at 0.14 eV below the valence band top. The reason of this broadening can be attributed to the delocalization of the $1b_1$ orbital of H_2O. Indeed, the charge of O_W pouring into H_W as reflected in the Mulliken charge population analysis in structure **II** (the charge of O_W decreases and that of H_W increase in comparison with the other two structures **I** and **III** as shown in Table 3.) If a hole appears on the surface after the photoabsorption of anatase TiO_2, then this hole possibly migrates to this H_2O molecule due to the oxygen charge and the energy levels position. This means that H_2O cation radical can appear on the surface more easily. This cation radical surely has the possibility to attack dye molecules on the surface. In order to make DSSC robust and effective, therefore, it is better to fabricate the DSSC under a low-humidity environment.

4. CONCLUSIONS

We have calculated the interfaces between the anatase TiO_2 (101) surface and bulk MeCN contaminated by ubiquitous H_2O, whose density corresponds to 0.5 M in the aim of fabricating durable DSSCs, by using first-principles density functional theory molecular dynamics.

MeCN is strongly adsorbed to the anatase (101) surface due to the back-donating effect, which induces the decrease of the band gap of TiO_2. In contrast to the previous calculations,[14,15] it is impossible for MeCN molecules to fully cover the (101) surface by MeCN (coverage $\Theta \approx 0.6$). There is a lot of space on the surface and potentially active space (Ti_{5C}) remains. However, it is found impossible for H_2O in bulk MeCN to dive into the unbound Ti_{5C} sites on the (101) surface kinetically because MeCN layer hinders H_2O from approaching the surface.

Although Ti_{5C} is not the adsorption site for H_2O in MeCN, it is hard to remove the water molecule adsorbed on the (101) surface before the surface is dipped into bulk MeCN because of the strong hydrogen bonds between H_W and O_{2C}. This structure has a slightly broadened $1b_1$ orbital of H_2O molecule, and the upper edge is located around just 0.14 eV below the valence band of TiO_2 at an average of three snapshots. Hence, this water molecule has more possibility to receive a hole possibly generated on the TiO_2 surface by irradiation. This means that the H_2O cation radical might appear on the surface, which has the possibility to attack the dye molecules adsorbed on the TiO_2 surface.

With these calculations, we demonstrate that it is better to remove H_2O on the TiO_2 surface before immersing the TiO_2 film into MeCN solvent. This implies that DSSCs should be fabricated under as low-humidity environment as possible to make them more durable.

■ ASSOCIATED CONTENT

Supporting Information. Optimized structures of one MeCN and H_2O molecule on the TiO_2 anatase (101) surface

with their adsorption energies and the magnified view around the H_2O molecule of each **I**, **II**, **III** system are also shown. This material is available free of charge via the Internet at http://pubs.acs.org.

AUTHOR INFORMATION

Corresponding Author
*E-mail: TATEYAMA.Yoshitaka@nims.go.jp.

ACKNOWLEDGMENT

This work was partly supported by KAKENHI 2054038 and 23340089. The calculations in this work were carried out on the supercomputer centers of NIMS, ISSP, The University of Tokyo, T2K-Tokyo, and T2K-Tsukuba.

REFERENCES

(1) O'Regan, B.; Grätzel, M. *Nature* **1991**, *353*, 737–740.
(2) Grätzel, M. *Nature* **2001**, *414*, 338–344.
(3) Hagfeldt, A.; Boschloo, G.; Sun, L.; Kloo, L.; Pettersson, H. *Chem. Rev.* **2010**, *110*, 6595–6663.
(4) Bergmann, R. B. *Appl. Phys. A: Mater. Sci. Process.* **1999**, *69*, 187–194.
(5) Chiba, Y.; Islam, A.; Watanabe, Y.; Komiya, R.; Koibe, N.; Han, L. *Jpn. J. Appl. Phys.* **2006**, *45*, L638–L640.
(6) Mohammad, K. N.; Péchy, P.; Renouard, T.; Zakeeruddin, S. M.; Humphry-Baker, R.; Comte, P.; Liska, P.; Cevey, L.; Costa, E.; Shklover, V.; Spiccia, L.; Deacon, G. B.; Bignozzi, C. A.; Grä1tzel, M. *J. Am. Chem. Soc.* **2001**, *123*, 1613–1624.
(7) Katoh, R.; Furube, A.; Kasuya, M.; Fuke, N.; Koide, N.; Han, L. *J. Mater. Chem.* **2007**, *17*, 3190–3196.
(8) Hara, K.; Horiguchi, T.; Kinoshita, T.; Sayama, K.; Arakawa, H. *Sol. Energy Mater. Sol. Cells* **2001**, *70*, 151–161.
(9) Takamuku, T.; Tabata, M.; Yamaguchi, A.; Nishimoto, J.; Kumamoto, M.; Wakita, H.; Yamaguchi, T. *J. Phys. Chem. B* **1998**, *102*, 8880–8888.
(10) Garabuleda, X.; Jaime, C.; Kollman, P. A. *J. Comput. Chem.* **2000**, *21*, 9901–908.
(11) Liu, Y.; Hagfeldt, A.; Xiao, X.-R.; Lindquist, S.-E. *Sol. Energy Mater. Sol. Cells.* **1998**, *55*, 267–281.
(12) Nazeeruddin, M. K; Kay, A.; Rodicio, I.; Humphry-Baker, R.; Muller, E.; Liska, P.; Vlachopoulos, N.; Grätzel, M. *J. Am. Chem. Soc.* **1993**, *115*, 6382–6390.
(13) Zhang, X.-T.; Taguchi, T.; Wang, H.-B.; Meng, Q.-B.; Sato, O.; Fujishima, A. *Res. Chem. Intermed.* **2007**, *33*, 5–11.
(14) Schiffmann, F.; Hutter, J.; VandeVondele, J. *J. Phys.: Condens. Matter* **2008**, *20*, 064206(8pp).
(15) Silva, da R.; Rego, L. G. C.; Freire, J. A.; Rodriguez, J.; Laria, D.; Batista, V. S. *J. Phys. Chem. C* **2010**, *114*, 19433–19442.
(16) Schiffmann, F.; VandeVondele, J.; Hutter, J.; Wirz, R.; Urakawa, A.; Baiker, A. *J. Phys. Chem. C* **2010**, *114*, 8398–8404.
(17) CPMD V3.12: IBM Research division, MPI Festkoerperforschung Stuttgart: http://www.cpmd.org
(18) Louie, S. G.; Froyen, S.; Cohen, M. L. *Phys. Rev. B* **1982**, *26*, 1738.
(19) Nosé, S. *J. Chem. Phys.* **1984**, *81*, 511. Hoover, W. G. *Phys. Rev. A* **1985**, *31*, 1695.
(20) Car., R.; Parrinello, M. *Phys. Rev. Lett.* **1985**, *55*, 2471.
(21) Sumita, M.; Hu, C.; Tateyama, Y. *J. Phys. Chem. C* **2010**, *114*, 18529–18537.
(22) LIDE, D. R., Ed. *CRC Handbook of Chemistry and Physics*, 83rd ed.; CRC Press: Boca Raton, London, New York, Washington DC, pp 3−10.
(23) Desiraju, G. R.; Steiner, T. *The Weak Hydrogen Bond: In Structural Chemistry and Biology*; Oxford University Press: New York, 2001, page 13.
(24) Jung, Y.-S.; Yoo, B.; Lim, M. K.; Lee, S. Y.; Kim, K.-J. *Electrochim. Acta* **2009**, *54*, 6286–6291.
(25) (a) He, Y.; Tilocca, A.; Dulub, O.; Annabella, S.; Diebold, U. *Nat. Mater.* **2009**, *8*, 585–589. (b) Li, W.-K.; Gong, X.-Q.; Lu, G.; Selloni, A. *J. Phys. Chem. C* **2008**, *112*, 6594. (c) Gong, X.-Q.; Selloni, A.; Batzill, M.; Diebold, U. *Nat. Mater.* **2006**, *5*, 665–670. (d) Tilocca, A.; Selloni, A. *J. Phys. Chem. B* **2004**, *108*, 4743–4751. (e) Tilocca, A.; Selloni, A. *J. Chem. Phys.* **2003**, *119*, 7445–7450. (f) Herman, G. S.; Dohnalek, Z.; Ruzycki, N.; Diebold, U. *J. Phys. Chem. B* **2003**, *107*, 2788–2795. (g) Nakamura, R.; Imanishi, A.; Murakoshi, K.; Nakato, Y. *J. Am. Chem. Soc.* **2003**, *125*, 7443–7450.
(26) (a) Tilocca, A.; Selloni, A. *Langmuir* **2004**, *20*, 8479–8384. (b) Mattili, G.; Filippone, F.; Caminitt, R.; Bonapasta, A. A. *J. Phys. Chem. C.* **2008**, *112*, 13579–13586. (c) Cheng, H.; Selloni, A. *Langmuir* **2010**, *26*, 11518–11525.